national accelerator laboratory

TM-239
1100.7

DESIGN OF PERSONNEL AND VEHICLE ACCESS LABYRINTHS

P. J. Gollon and R. A. Carrigan, Jr.

May 5, 1970

1. Monte Carlo Calculation of Neutron Attenuation of Main-Accelerator Labyrinths

The neutron flux attenuation of the main-ring major and minor vehicle entrances and service-building labyrinths were calculated using a Monte Carlo neutron transport program. The program ZEUS ALB. 5, written by François Gervaise and Marguerite-Marie d'Hombres (Centre d'Etudes Nucleaires de Fontenay-aux-Roses), has the ability to randomly generate monoenergetic neutrons (energy chosen by the user) and transport them through a labyrinth of nearly arbitrary shape. Reflection of the neutrons from the concrete walls of the labyrinth is treated by the albedo method.[1] A detailed description of the program may be found elsewhere.[2,3]

All linac, booster, and main-ring labyrinths were designed to have an attenuation of 5×10^{-7}, consistent with the attenuation of the earth shielding.[4]

The major vehicle entrance (Fig. 1) consists of a semicircular tunnel with an 8 ft × 8 ft cross section. The radius of curvature of the inner wall is 50 ft. Only particles produced in a backward direction from the proton beam can travel down the curved labyrinth for any

Operated by Universities Research Association Inc. Under Contract with the United States Atomic Energy Commission

significant distance. At the far end of the labyrinth there is a hoist shaft, stairway, and elevator.

For purposes of calculation, a beam loss was assumed to occur at a point on the beam line, just in front and upstream of the entrance to the labyrinth, as shown in Fig. 1. The calculated neutron fluxes at various distances down the centerline of the tunnel from the loss point are shown in Fig. 2. After a short transition region in which the loss point can be seen directly, the attenuation per foot of tunnel increases and remains constant throughout the curved region. The effect of the short straight section of tunnel before the shaft, and the sharp decrease in flux around the 90° bend formed by the shaft can also be seen. The overall attenuation of the labyrinth is defined as

$$A = \frac{\text{neutron flux into labyrinth opening}}{\text{neutron flux at floor of head house}} = 10^{-8}.$$

Thus, this design which was dictated by architectural considerations is quite adequate for the anticipated main-ring beam losses.

The initial design of the minor vehicle accesses (Fig. 3) consisted of 170° of 6 ft $\times$ 8 ft tunnel with a 12-ft inner radius of curvature, followed by a short reverse curve and a straight ramp section which rises to the surface. The results of a Monte Carlo calculation for this labyrinth (Fig. 4) indicated that its attenuation of 2×10^{-7} would be sufficient.

The inner radius of the semicircular section of this labyrinth was subsequently increased from 12 ft to 25 ft. The length of the straight part remained unchanged.

The increase in radius of curvature to 25 ft was more than compensated for by the increased length of the semicircle. This may be seen by noting from Fig. 4 that the attenuation of $\pi(12 + 3)$ ft = 47 ft of 12 ft tunnel is 4×10^{-5}. The corresponding distance in a 25-ft inner radius tunnel is $\pi(25 + 3) = 88$ ft. Figure 2 indicates that 88 ft of tunnel of a larger cross section and 50-ft inner radius has an attenuation of 8×10^{-5}. The remaining factor of 2 will be more than made up by the fact that the actual inner radius of the tunnel is 25, not 50 ft.

The last labyrinth calculated using ZEUS was the personnel access from each of the 24 service buildings to the main-accelerator enclosure. This is a 3-legged labyrinth 3-ft wide × 9-ft high (Fig. 5) with centerline measurements of 24, 18, and 30 ft. (Distances are measured parallel to the average rise of the stairs.) Two calculations were made for this labyrinth--one with two 3-ft cul-de-sacs, the other without cul-de-sacs. The results are shown in Fig. 6. Each cul-de-sac gives an additional neutron flux attenuation of three. The overall attenuation of the labyrinth without cul-de-sacs is 2×10^{-7}, as built with one cul-de-sac which houses a sump, the attenuation is 7×10^{-8}. Again, this is more than adequate for the anticipated losses.

2. Neutron Attenuation of Linac and Booster Access Labyrinths

a) Linac 200-MeV Labyrinth

The attenuation of the 3 ft × 9 ft, 4-leg labyrinth (Fig. 7) at the 200-MeV switchyard was calculated using the results of the Monte Carlo ZEUS ALB. 5 calculation described above for the main-accelerator service-building access labyrinths.

The lengths and flux attenuations of the various legs as read from the appropriate portions of Fig. 6 above are

Table I.

Leg #	Leg Length Feet	Does It Start With A Cul-De-Sac?	Attenuation
1	9.5	no	0.25
2	15.0	yes	1.4×10^{-3}
3	9.0	yes	1.5×10^{-2}
4	4.5	yes	7.0×10^{-2}

Hence, the overall attenuation which is equal to the product of the attenuations of the various legs is

$$\text{Atten} = 4 \times 10^{-7}.$$

This number is smaller than the design criterion of 5×10^{-7}. Therefore, this attenuation is considered adequate.

b) Booster Personnel Access Labyrinths

The neutron attenuation of the 3-legged 4 ft × 8 ft labyrinths between the booster enclosure and booster galleries (Fig. 8) was also calculated using results from the above Monte Carlo results for the main-accelerator service-building access labyrinths. The difference in cross-sectional areas of the two labyrinths was taken into account by scaling the true centerline distance of the labyrinth, L, by the square root of the cross-sectional areas of the two tunnels:

$$L_{eff} = L \times \sqrt{\frac{\text{Area (MR)}}{\text{Area (Boost)}}} = L \times \sqrt{\frac{9\times 3}{8\times 4}} = 0.92L.$$

This use of the effective length, L_{eff}, has been justified elsewhere.[5] The attenuation of the various legs as read from Fig. 6 are as follows:

Leg	Leg Length Feet	Effective Length Feet	Attenuation
1	11.5	10.5	0.22
2	22	20.2	7×10^{-4}
3	26	23.9	6×10^{-4}

The neutron attenuation was calculated at the doorway between the 8-ft long passageway in front of the fan room and the stairs down to the booster enclosure.

The overall attenuation, equal to the product of the attenuations for the three legs, is

$$\text{Atten} = 9.2\times 10^{-8}.$$

As this number is smaller than the design attenuation of 5×10^{-7}, the labyrinth attenuation is considered adequate.

c) Vehicle Access Labyrinth to Booster Enclosure

The S-shaped vehicle access labyrinth to the booster (Fig. 9) contains three curves with an inner radius of 25 ft, three straight transition sections, two cul-de-sacs, and a vertical shaft. The attenuation of each of these components can be calculated or estimated in the same manner as in the preceeding examples. In order to use the results of the main-accelerator minor vehicle entrance calculation, we must again compensate for the increased cross-sectional area of this labyrinth by using the "effective length":

$$L_{eff} = \sqrt{\frac{8 \times 8}{8 \times 10}} * L = 0.89 L.$$

The attenuation provided by each component is then:

	Length	Effective Length	Attenuation
straight	70 ft	63 ft	0.01
curved	124 ft	111 ft	$\approx 4 \times 10^{-5}$
cul-de-sac (2)	--	--	0.1
hoist shaft	17.5 ft	--	0.015

The resulting neutron flux attenuation is 6×10^{-10}. This is probably an overly optimistic figure because the large attenuation of the curved sections is diluted by their relatively short length. However, even if this effect makes the above estimate too optimistic by one or even two orders of magnitude, there is still an ample safety factor above the design attenuation of 5×10^{-7}.

Acknowledgment

The ZEUS ALB. 5 program package was very kindly supplied to us by the Centre d'Etudes Nucleaires de Fontenay-aux-Roses.

REFERENCES

[1]R. E. Maerker, F. J. Muckenthaler, Calculation and Measurement of the Fast-Neutron Differential Dose Albedo for Concrete, Nucl. Sci. Eng. 22, 465 (1965).

[2]F. Gervaise, M-M. d'Hombres, Variante du Programme ZEUS Apliquie à des Problemes de Tunnels: Programme ZEUS ALB. 5 et Programmes Auxiliares, Centre d'Etudes Nucleaires de Fontenay-aux-Roses Note CEA-N-933, 1968.

[3]M-M. d'Hombres, C. Devillers, F. Gervaise, B. de Sereville, Ph. Tardy-Joubert, Propagation des Neutrons dans les Tunnels d'Acces à un Accelerateur de Haute Energie à Protons, GES.68.02-AIR. 41-NC; SPR/SI 162-AS-13, 1968.

[4]M. Awschalom, Linac Shielding: Expected Beam Losses, Design Criteria, Tolerable Beam Losses, Radioactivation and Remanent Exposure Rate, Dose Rate to Beam-Loss Monitors, National Accelerator Laboratory Internal Report TM-236, May 5, 1970, and TM in preparation.

[5]R. E. Maerker and F. J. Muckenthaler, Monte Carlo Calculations. . . of One- and Two-Legged Square Concrete Open Ducts. . . , Nucl. Sci. Eng. 27, 423 (1967).

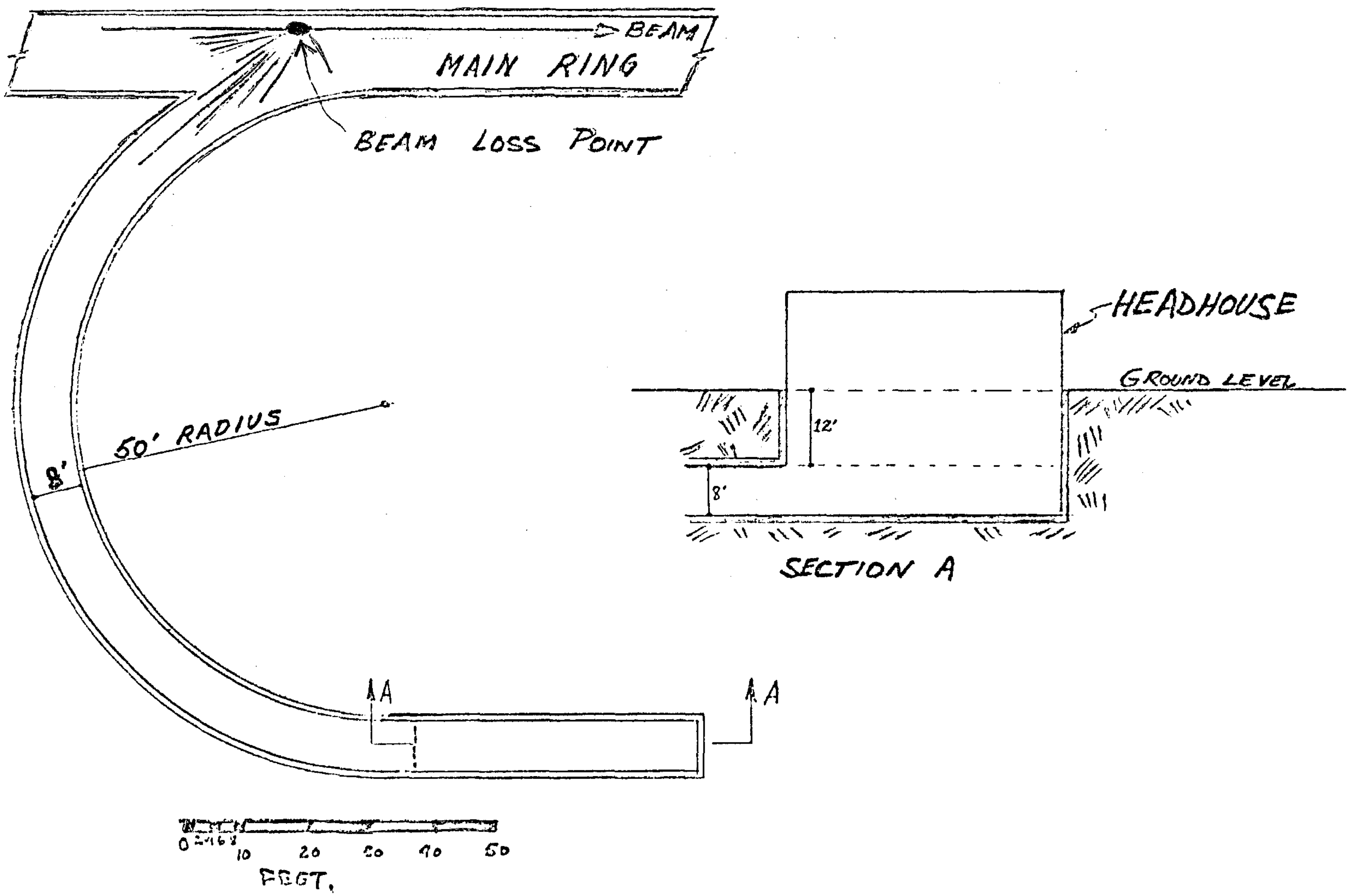

Figure 1. Major vehicle entrance to main accelerator enclosure. The stairs, elevator and hoist shaft leading down from the head house are not shown in the drawing, and were idealized into a single open shaft for purposes of calculation.

Figure 2

Neutron flux in the major vehicle entrance, (Fig. 1) as a function of distance from the assumed beam loss point. The vertical bars indicate the statistical errors in the Monte Carlo calculations. The average flux incident on a head house wall is also shown. All distances are measured down the center of the labyrinth.

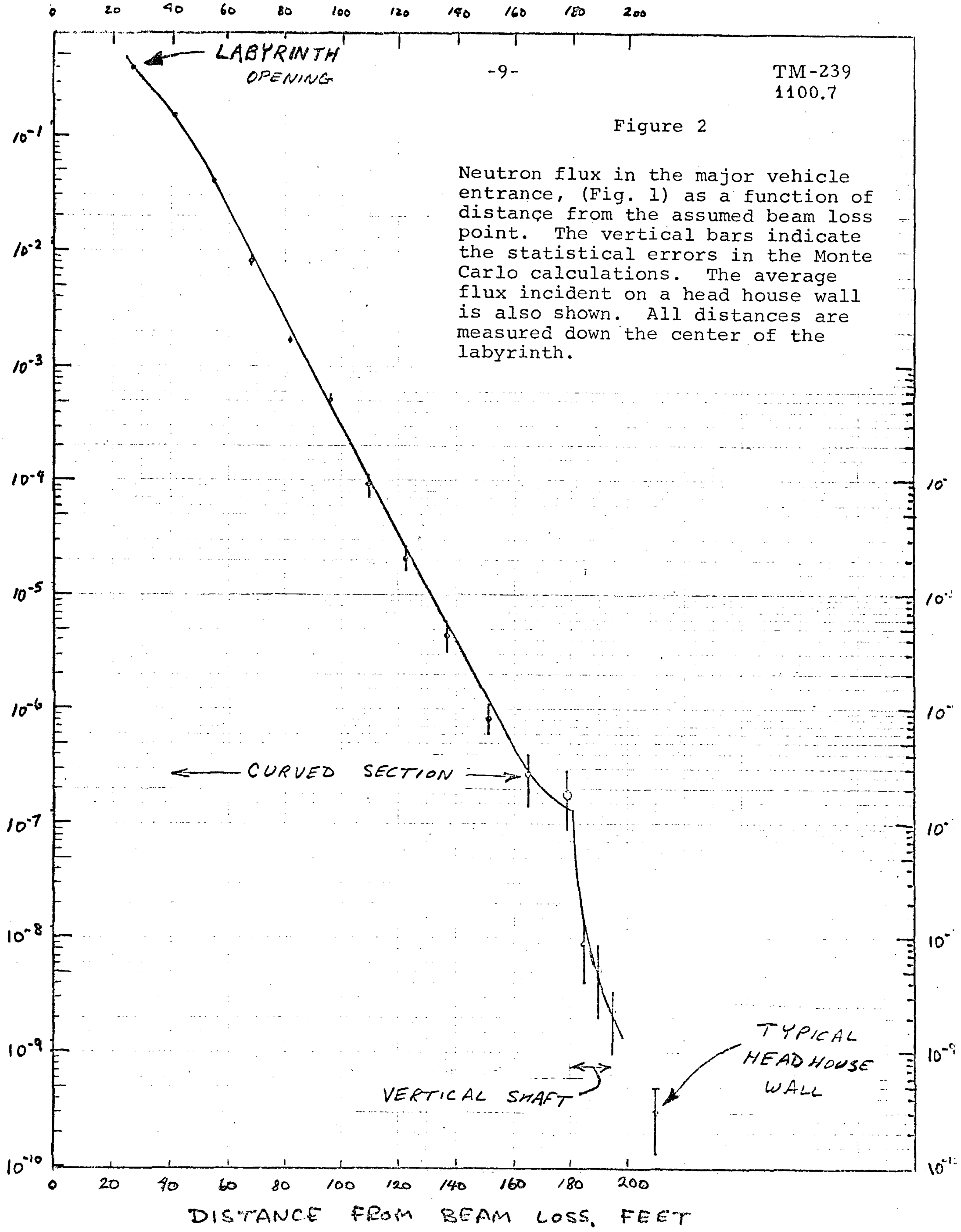

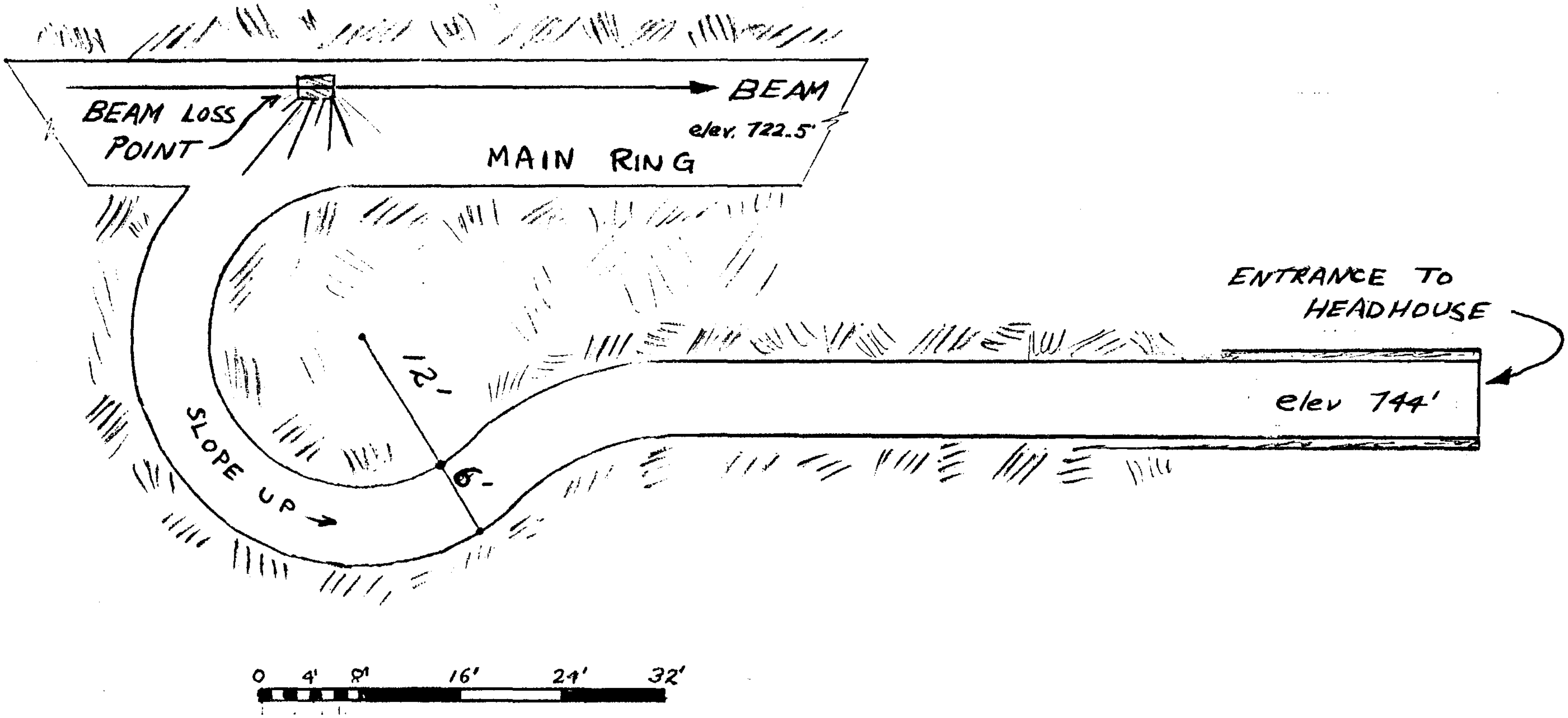

Figure 3. Initial design of minor vehicle entrance to main accelerator enclosure. The ramp runs from ground level (744') down to the level of the main accelerator enclosure floor (722.5').

TM-239
1100.7

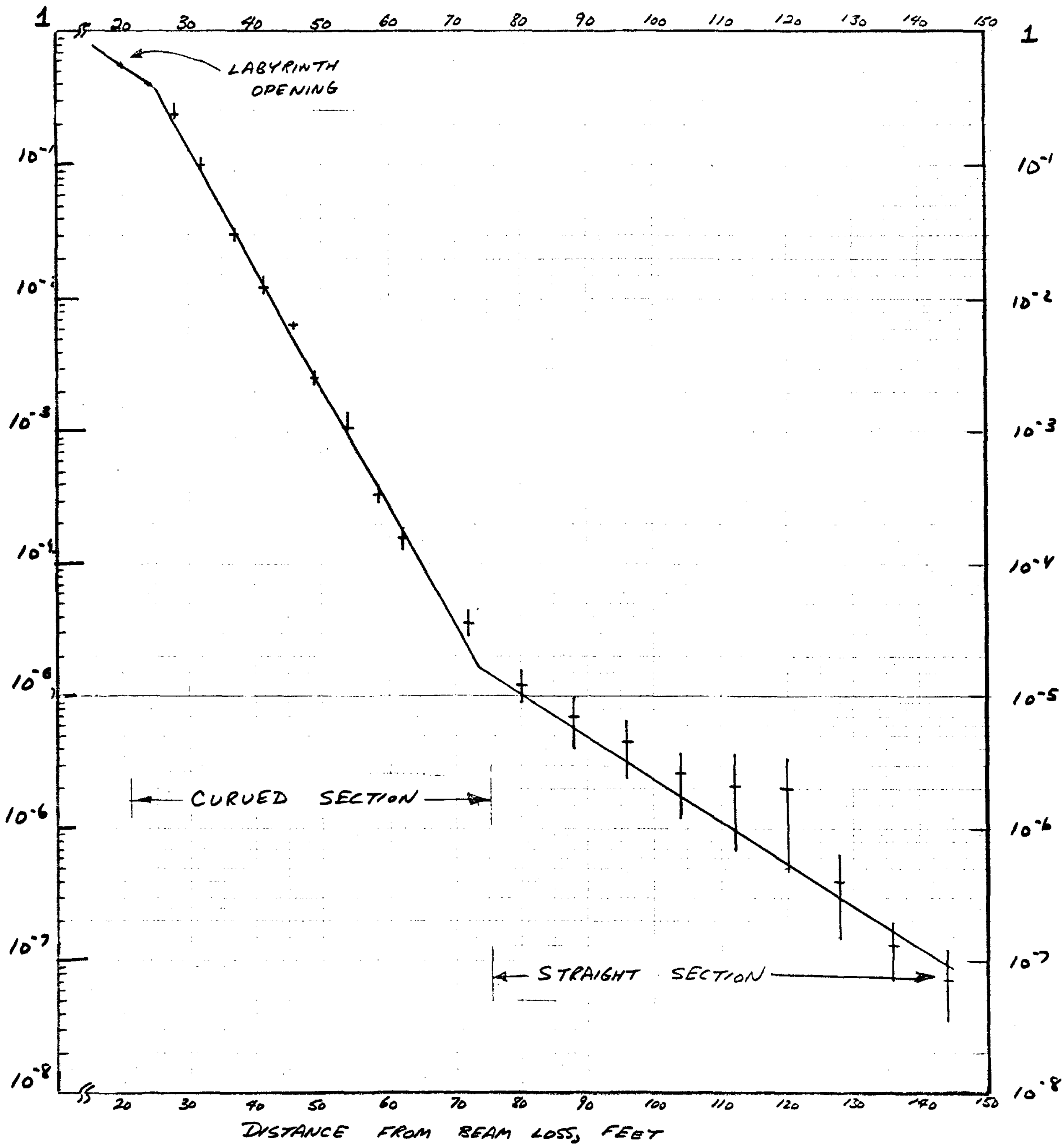

Figure 4. Neutron flux in the minor vehicle entrance shown in Figure 3 as a function of distance from the assumed beam loss point.

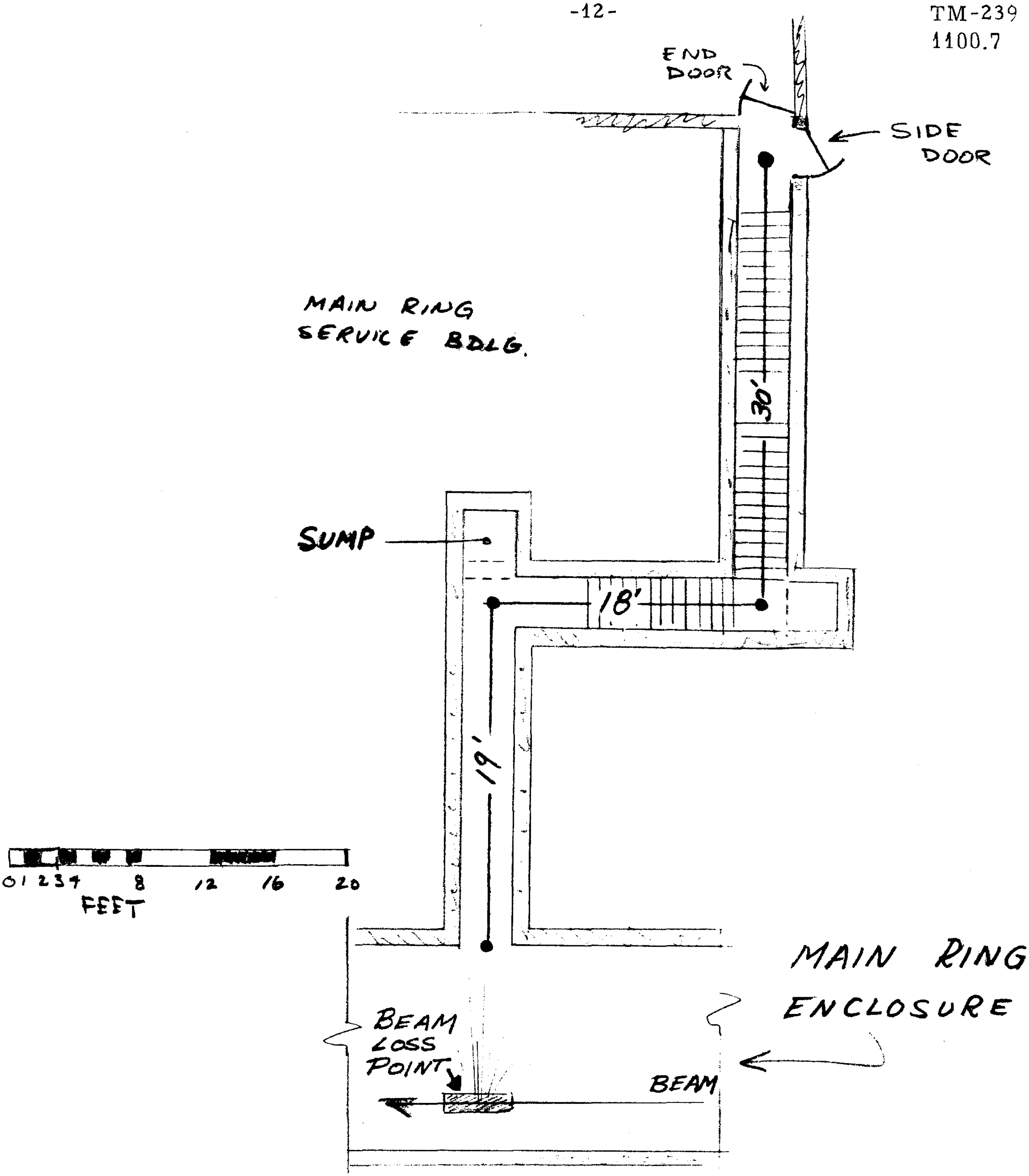

Figure 5. Personnel access labyrinths between main accelerator enclosure and service buildings. Distances in the second and third legs are measured parallel to the average rise of the stairs.

Neutron flux in the personnel access labyrinth of Fig. 5 as a function of distance from the assumed **beam loss** point. The fluxes incident **on the** side and end doors at the **top of** the labyrinths are also shown. **Calculations were made for this labyrinth with and without cul-de-sacs after the first and second legs.**

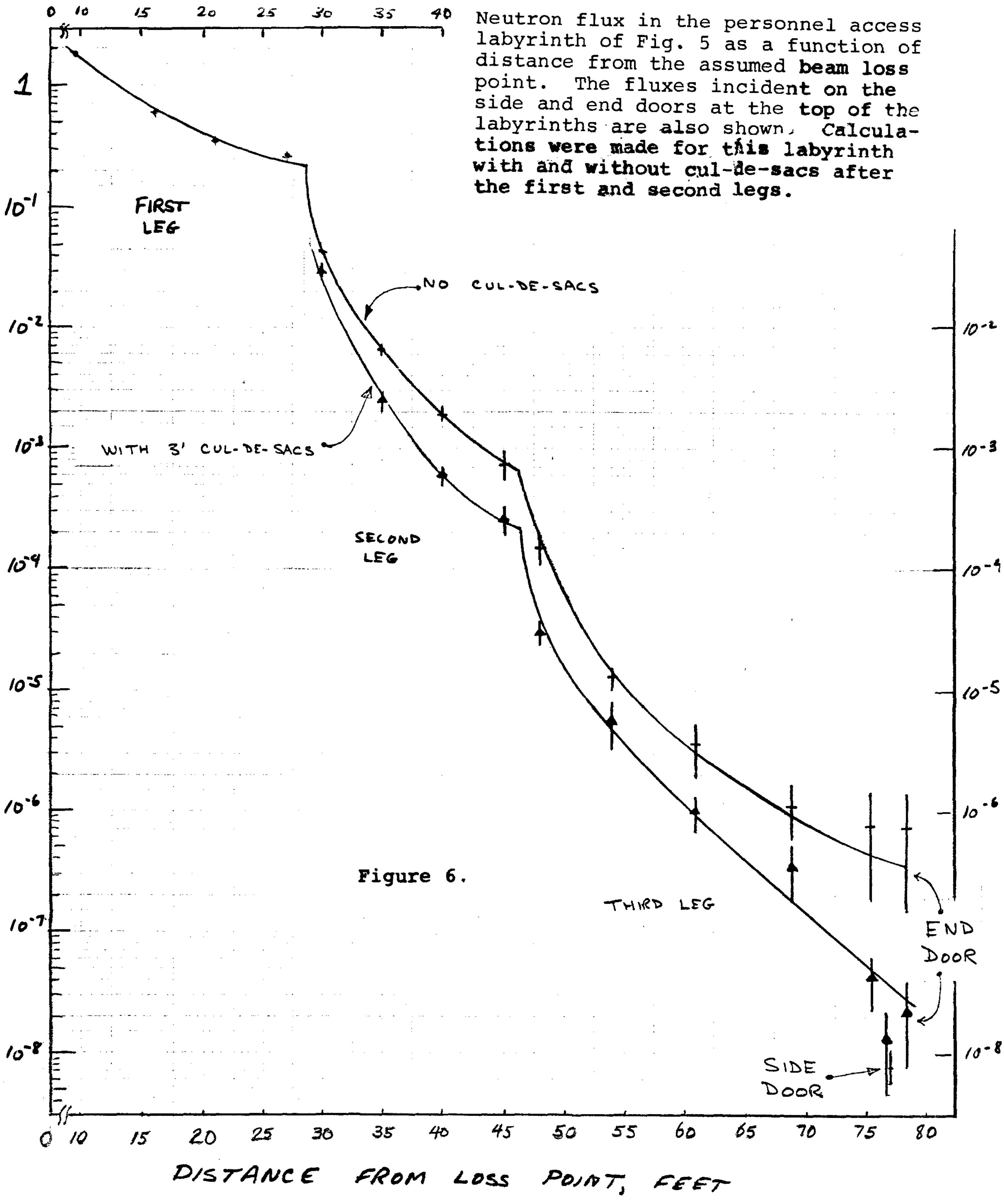

Figure 6.

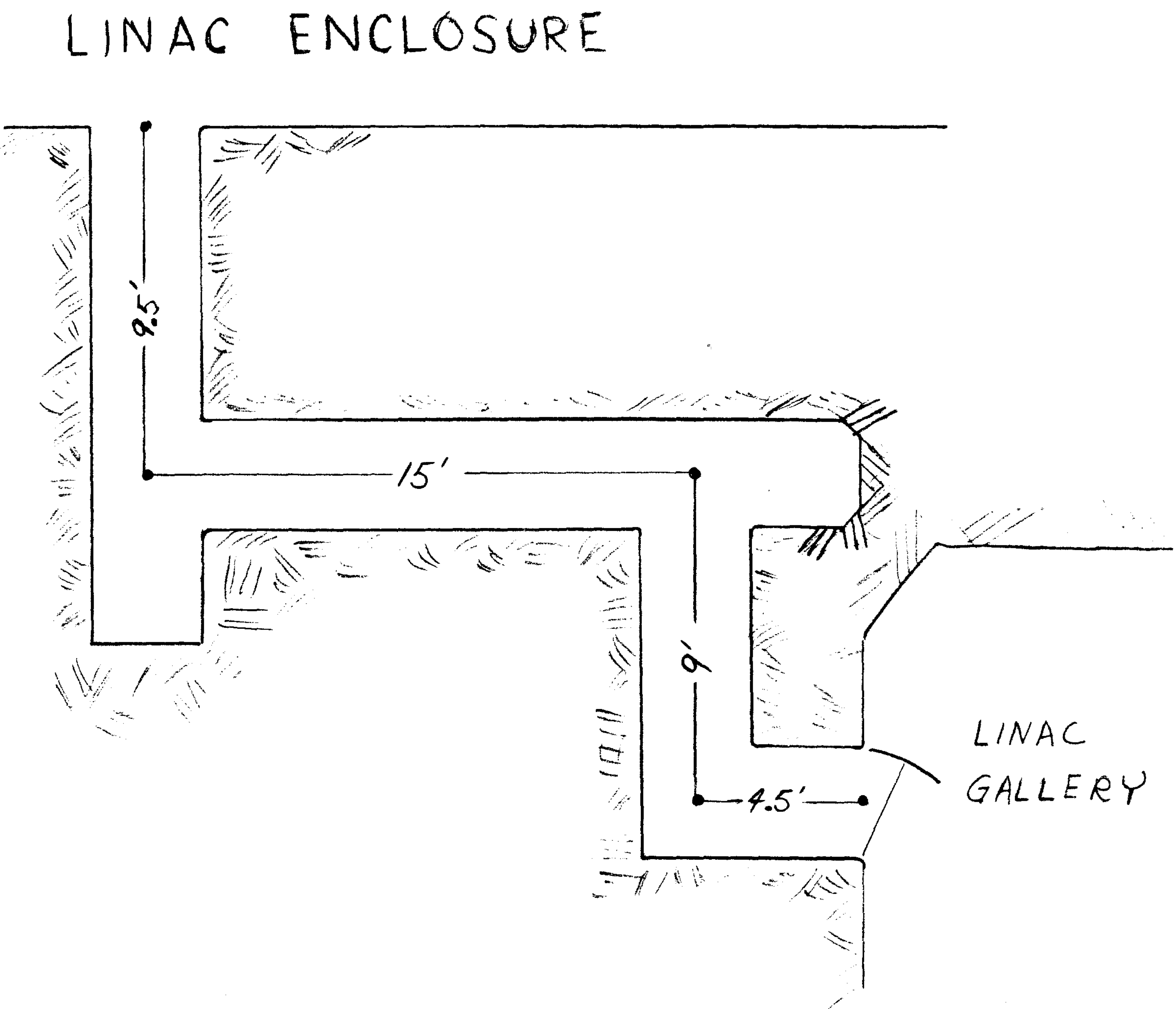

Figure 7. Personnel access labyrinths between the linac gallery and 200 MeV end of the linac enclosure.

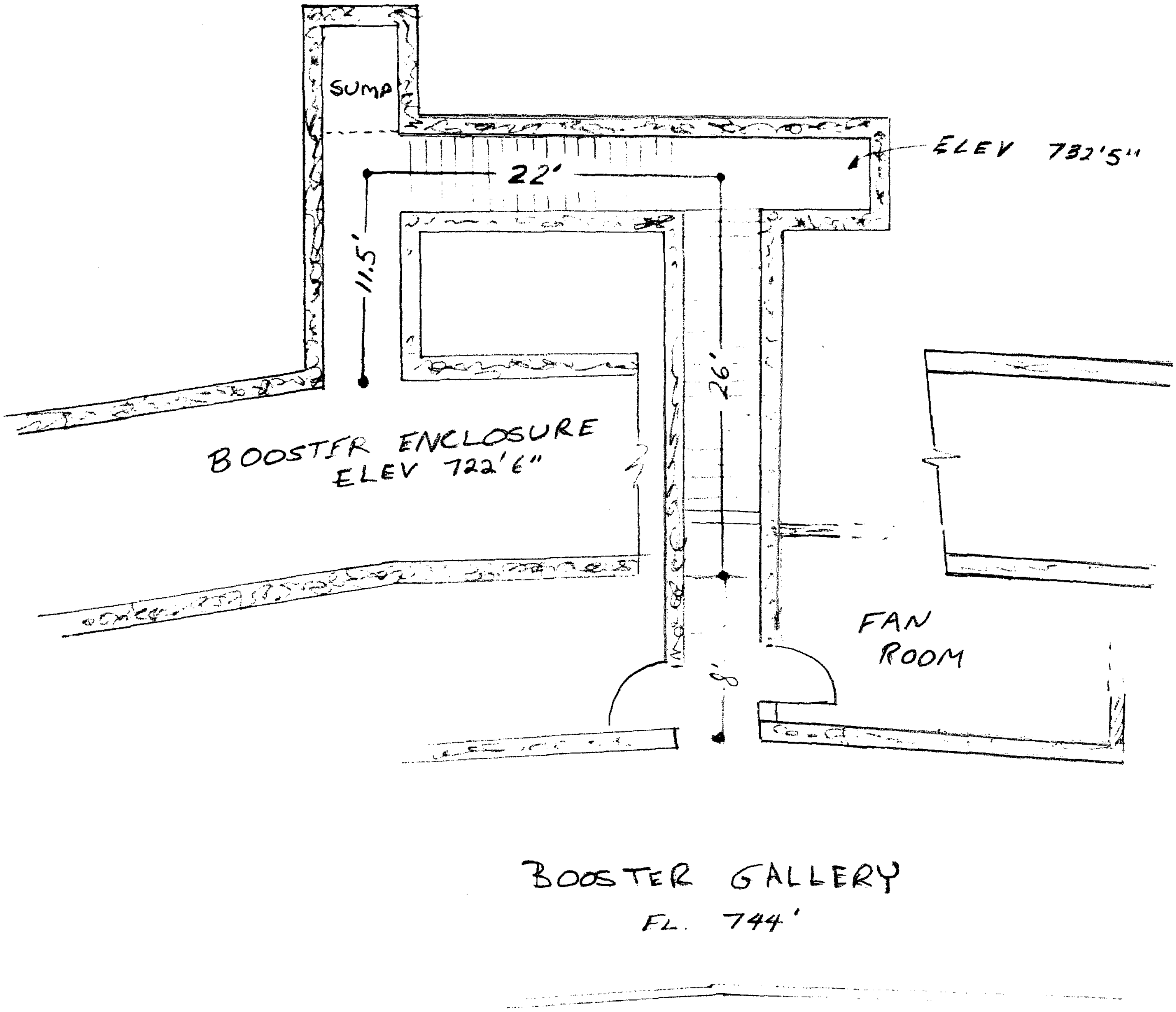

Figure 8. Personnel access labyrinth between the booster enclosure and booster gallery.

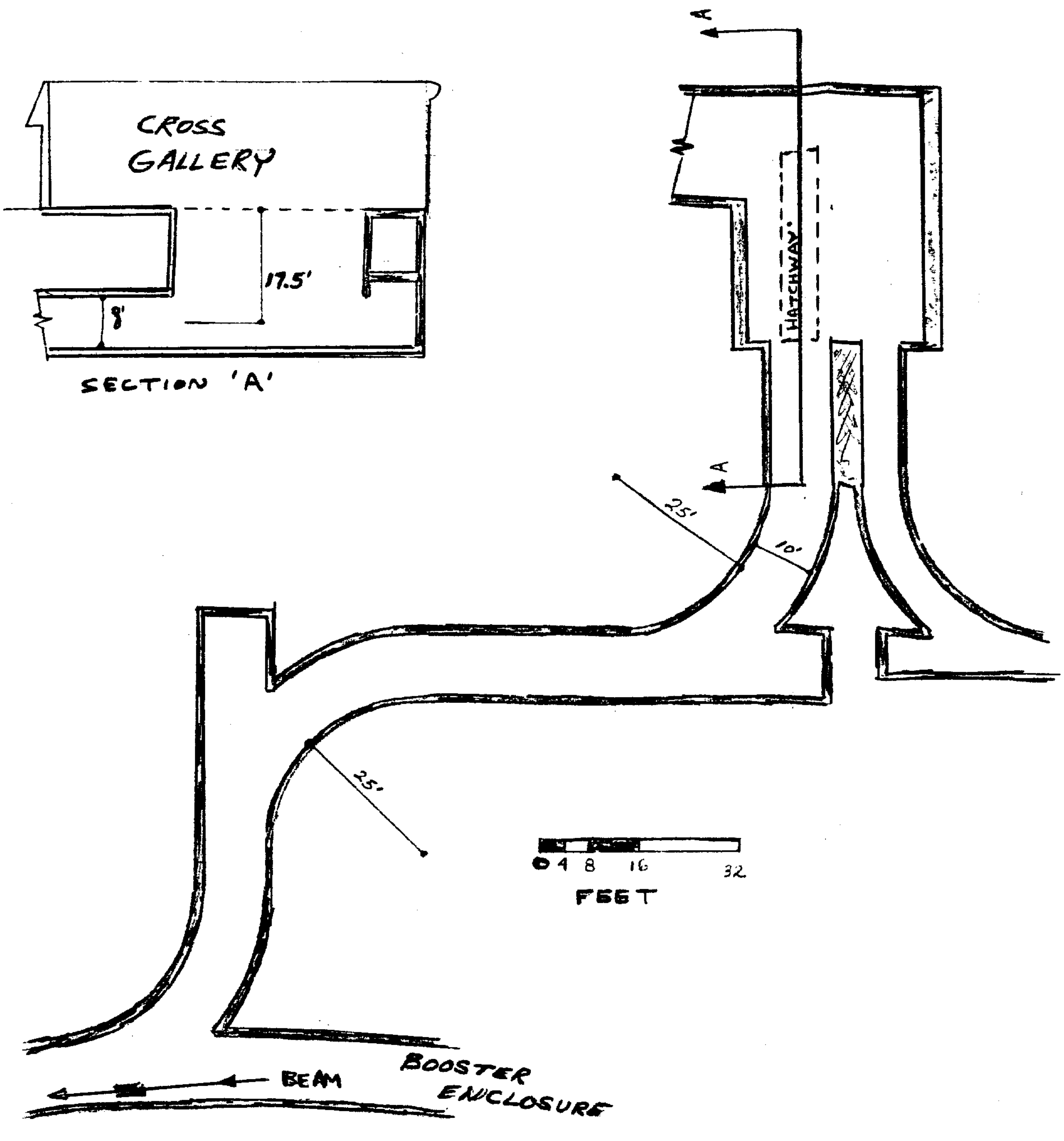

Figure 9. Vehicle access labyrinth from cross gallery to booster enclosure.